HamSCI Workshop 2019
Case Western Reserve University
March 22-23, 2019

Crazy Antennas

Dr. Bob Romanofsky
Senior Technologist
Communications and Intelligent Systems Division
NASA Glenn Research Center
Cleveland, OH

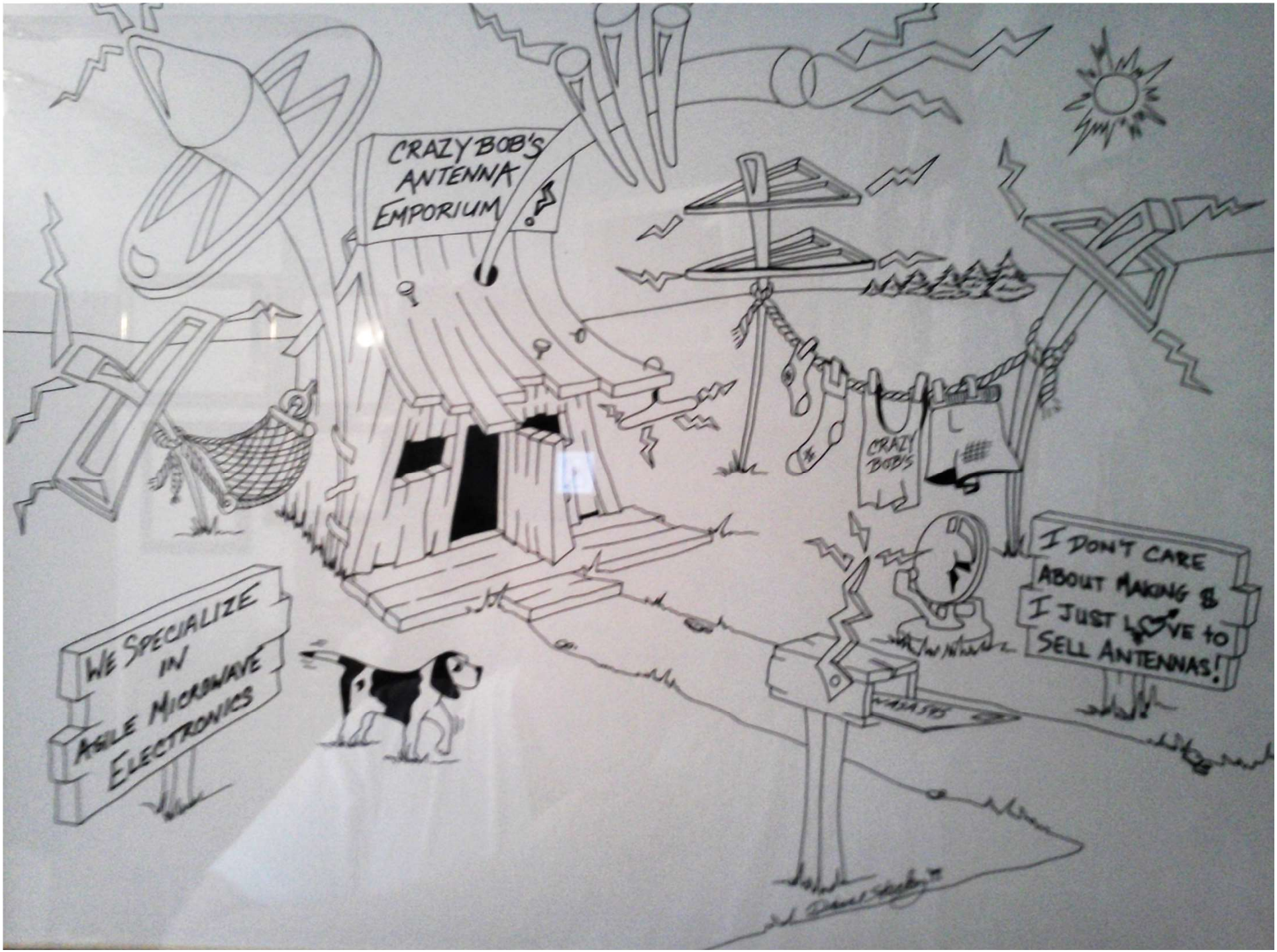
CRAZY BOB'S ANTENNA EMPORIUM
CRAZY BOB'S
WE SPECIALIZE IN AGILE MICROWAVE ELECTRONICS
I DON'T CARE ABOUT MAKING $ I JUST LOVE TO SELL ANTENNAS!

Abstract

Everyone here is familiar with traditional antennas, time-honored favorites like dipoles and solid parabolic reflectors. But occasionally, circumstances call for something peculiar. This paper will describe a number of unusual antennas for particular communications scenarios that have been developed at the NASA Glenn Research over the past decade or so. The list includes:

- K-band scanning ferroelectric reflectarray;
- UHF "Vivaldi" for cellular connectivity to unmanned aerial vehicles;
- Ku-band array that develops a top-hat pattern to feed a zone plate antenna;
- Active antenna that toggles between Iridium and GPS bands;
- VHF hybrid spiral/dipole for orientation determination on Venus;
- Ku-band deployable reflector that strongly resembles a giant beach ball,
- Combination Ka-band parabolic reflector and 1550 nm telescope called the "teletenna."

Design strategy and performance results will be included, and trends towards cognitive antennas will be discussed.

Scanning Ferroelectric Reflectarray [1]

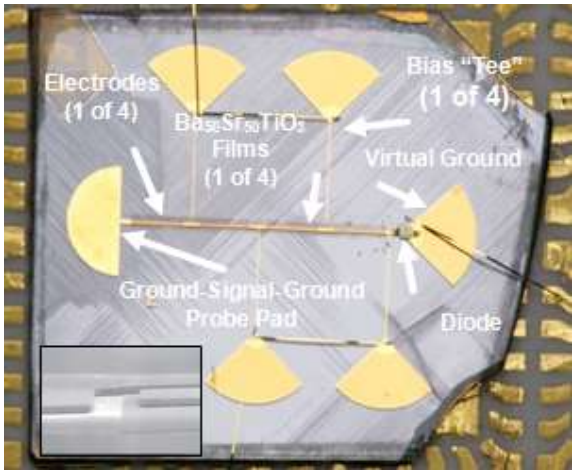

Hybrid X-band ferroelectric/semiconductor phase shifter on 0.5 mm thick lanthanum aluminate. The device is 10 mm X 9 mm. The 1.2 mm long G-S-G pad is sacrificed (sawed) after characterization, so final size is about 9 X 9 mm2. Each λg/4electrode produces ≈40° of phase shift. Inset shows SEM of partial electrode.

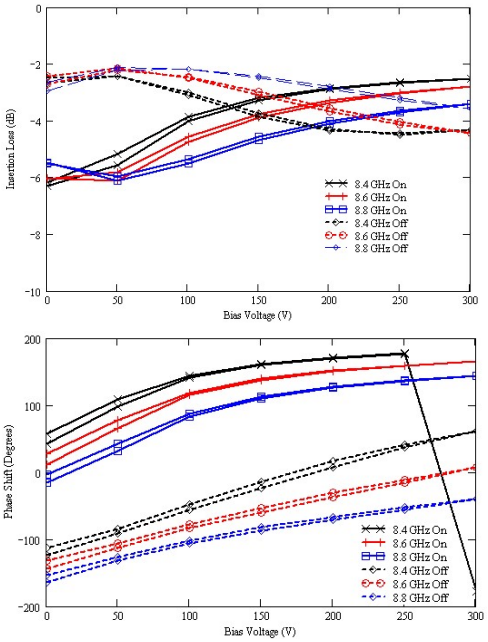

Measured insertion loss and phase of hybrid ferroelectric/ semiconductor phase shifter as a function of bias voltage on the ferroelectric section and switch state.

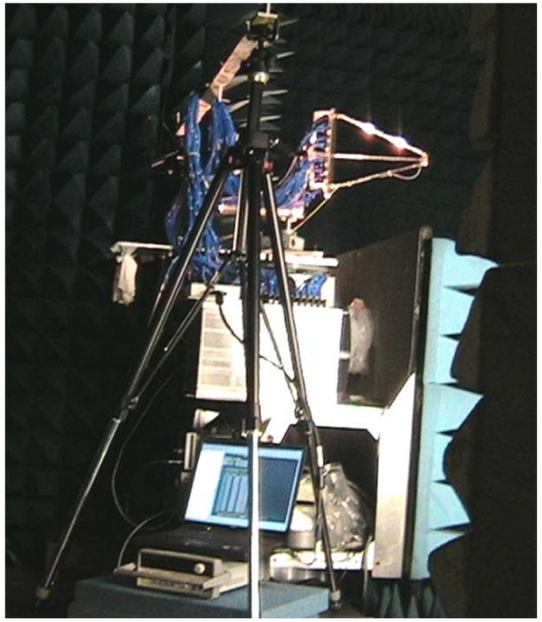

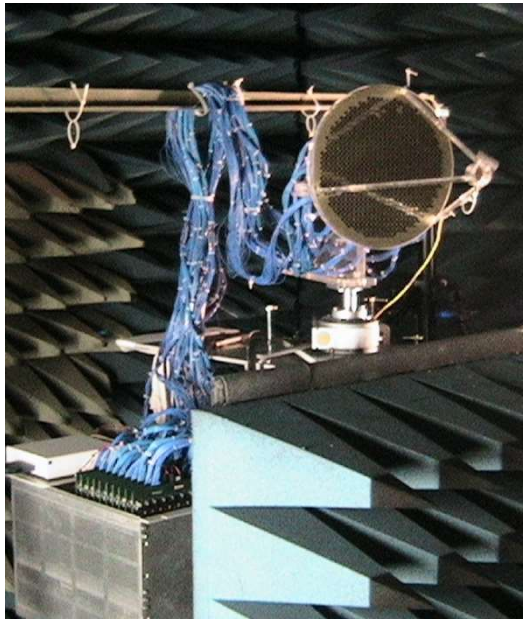

Testing the 615 Element K-band Reflectarray and Low Power Controller in NASA Glenn's Far Field Chamber

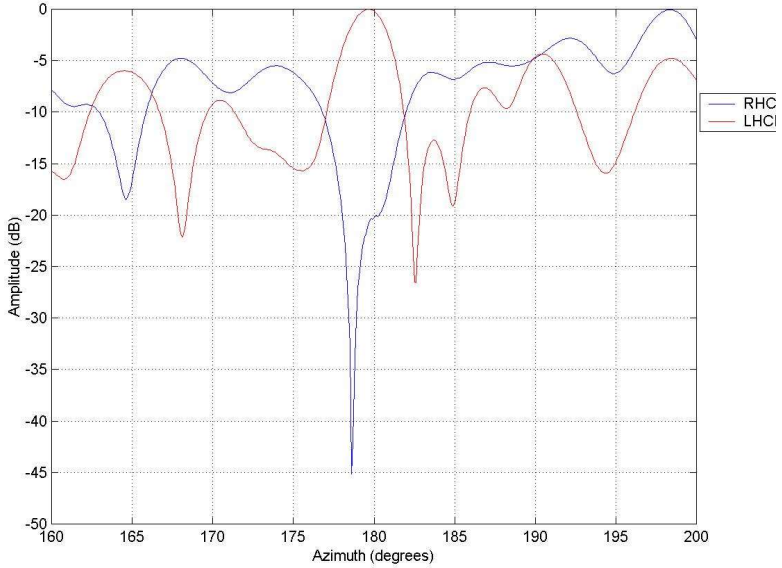

Measured Ferroelectric Reflectarray Antenna Pattern at 19 GHz

700 MHz to 2 GHz Vivaldi Proposed for Cellular Control of Unmanned Aerial Vehicles [2]

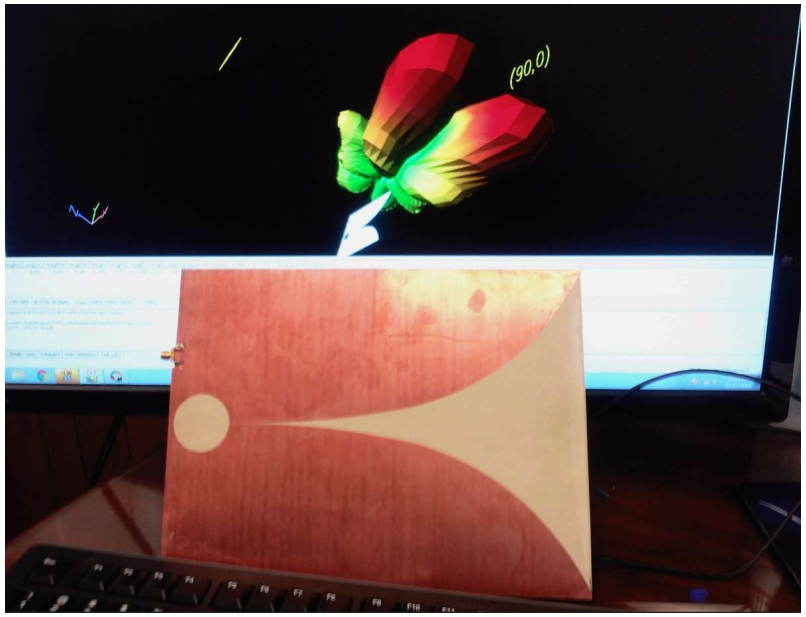

Simulated pattern at 2 GHz (background). The discontinuity at θ=90°,Φ=0° is an artifact of the finite ground plane but infinite substrate that was used in the model. Fabricated copper antenna on low-loss Teflon substrate (foreground) [3]

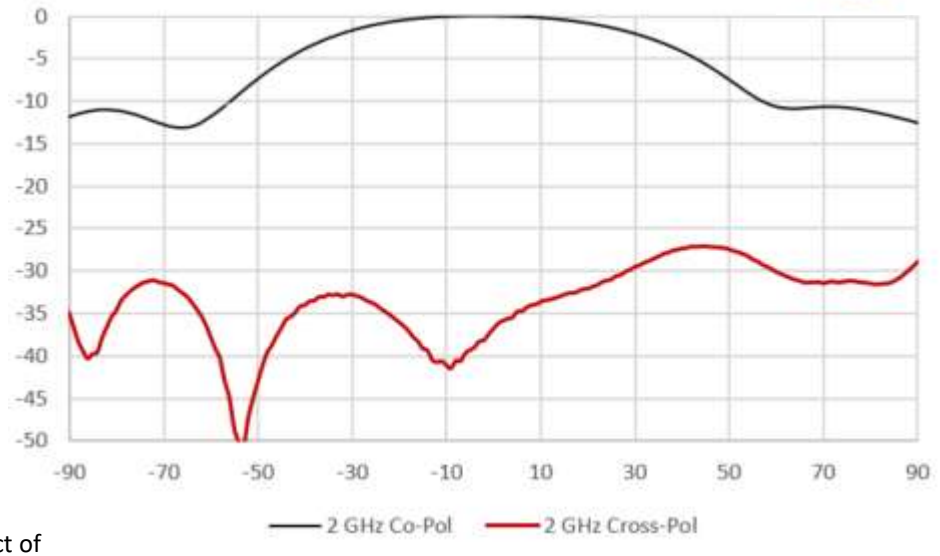

Measured far-field pattern at 2.0 GHz. The pattern at 1.7 GHz is indistinguishable.

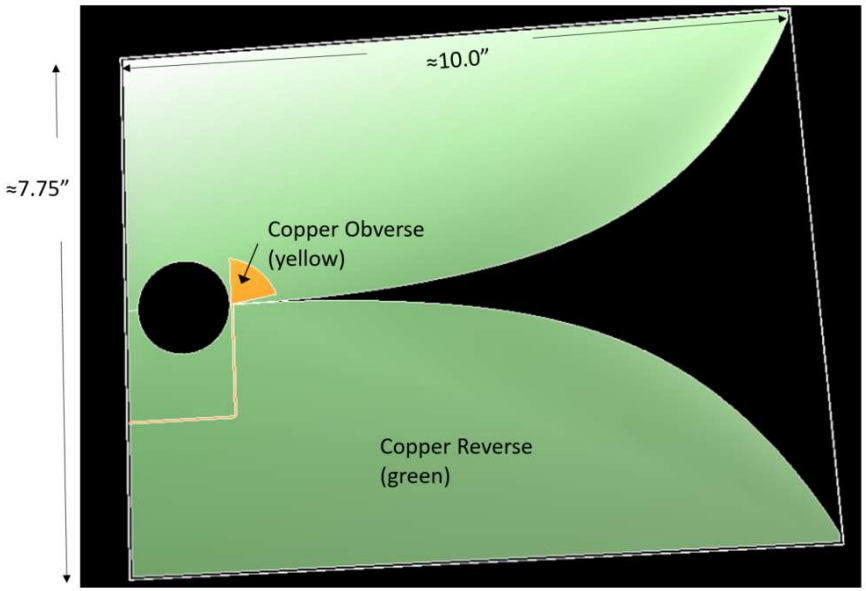

Design, with dimensions, showing both sides – the feed and radiator

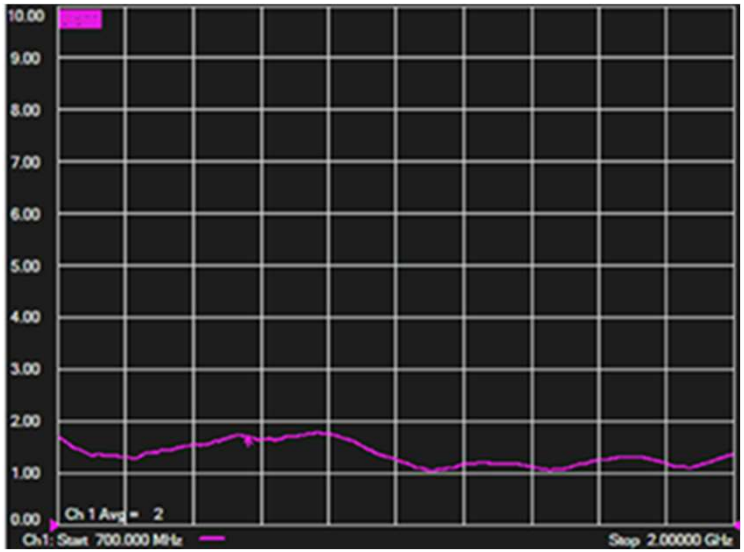

Measured VSWR – better than 2:1 from 700 MHZ to 2000 MHz

Synthesized Antenna for "Top-Hat" Radiation Pattern for Zone Plate Antenna [4]

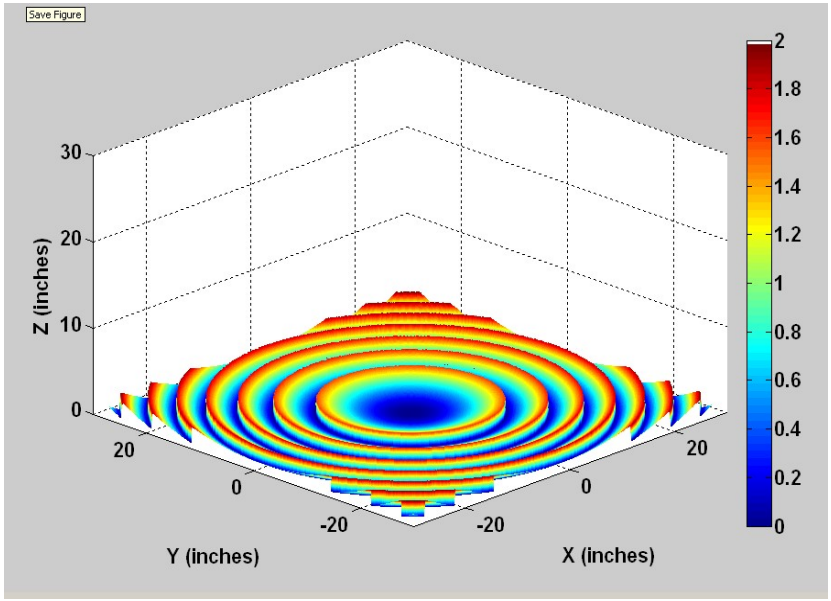

Model of 5 foot diameter "Zone Plate Antenna." The concentric rings are ½ wavelength steps at ≈ 12 GHz and the aperture forms a thin replacement for a parabolic reflector

Typical attenuator location corresponding to table on lower left; element # 1

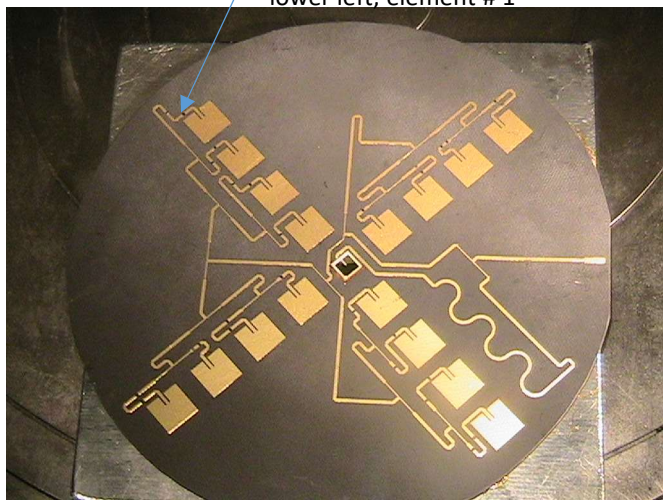

12 cm Uniform Amplitude Taper Array Feed for 1.5 m diameter Zone Plate Antenna

Autocorrelation of white noise at the output of the antenna is a sinc function. Thus for a band-limited system of 400 MHz, for example, the correlation time is approx. 2.5 ns. Since the ZPA induces a delay of 0.27 ns per ring by design, partial correlation of white noise may be present, resulting in some destructive interference of the noise signal

Synthesized element values using Woodward-Lawson method [5] corresponding to the pattern at right

Element #	1	2	3	4	5	6	7	8	9
Amplitude	0.026	0.086	0.156	0.219	0.756	0.219	0.156	0.086	0.026
Phase (degrees)	180	0	180	0	0	0	180	0	180

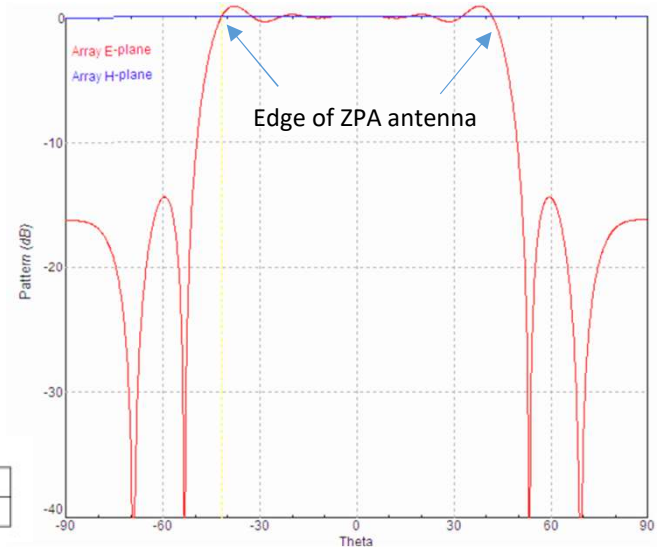

Modeled pattern at 11.7 GHz to uniformly illuminate 1.5 m ZPA

Voltage Tunable Low-Signature L-Band Antenna

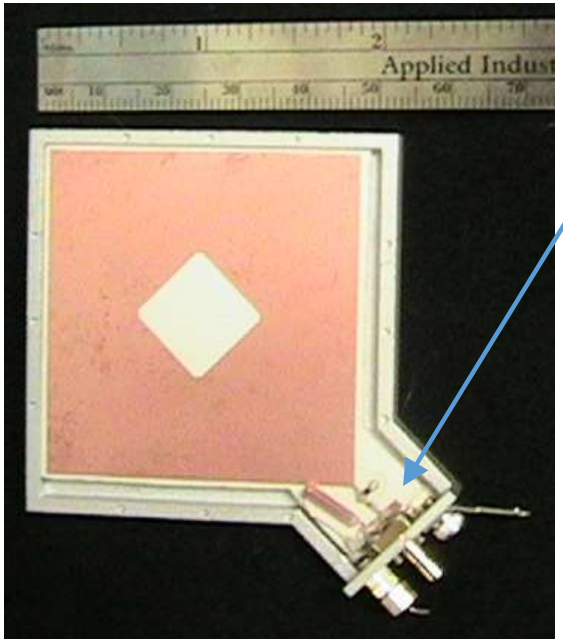

Resonant patch. Note that the antenna is only about ¼ wavelength long

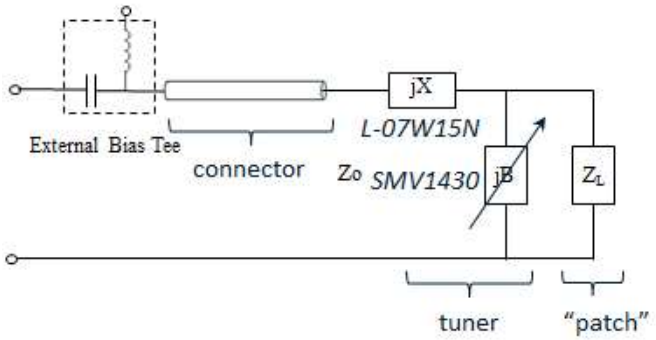

Tuning/Matching Circuit. SMV1430 is a varactor

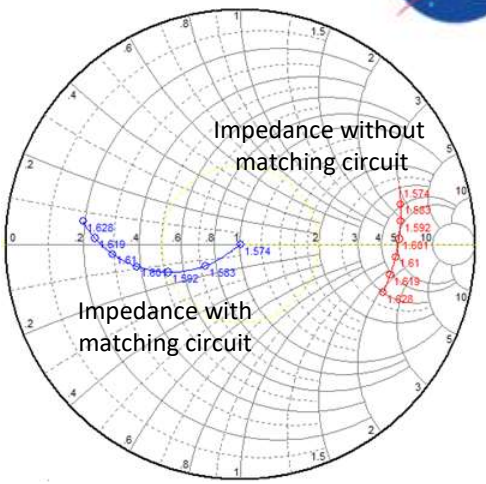

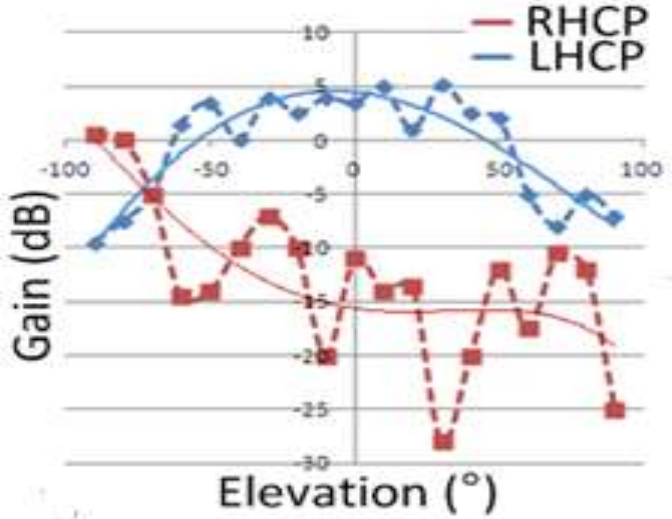

Measured far-field pattern at ≈mid-band

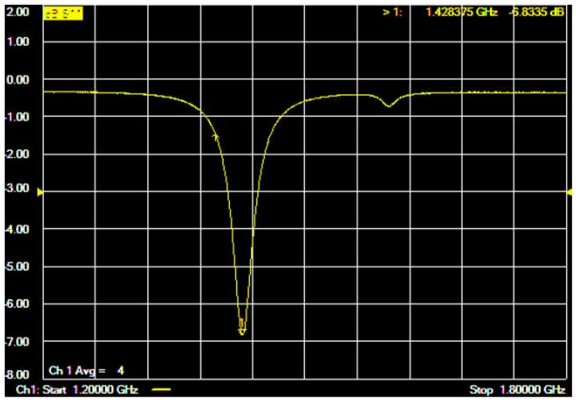

Measured return loss with 0 Volts Bias

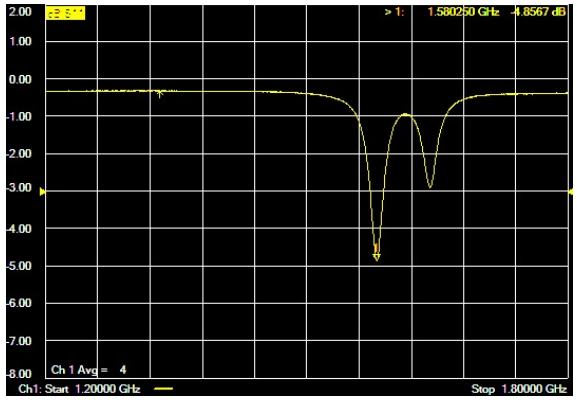

Measured return loss with 8 Volts Bias

The antenna's center frequency tunes between ≈1.4 and ≈1.6 GHz and covers GPS L1 and the high end of the Iridium band.

VHF Hybrid Spiral/Dipole Orientation Determining Antenna [7]

A normalized RHCP wave propagating along the **z** axis.

$$\boldsymbol{E} = (\mathbf{x} - j\mathbf{y})\, e^{-j\beta z}\, e^{-j\omega t}$$

It is a property of a circularly polarized antenna that a physical rotation of Ψ degrees results in a far-field phase shift of Ψ degrees

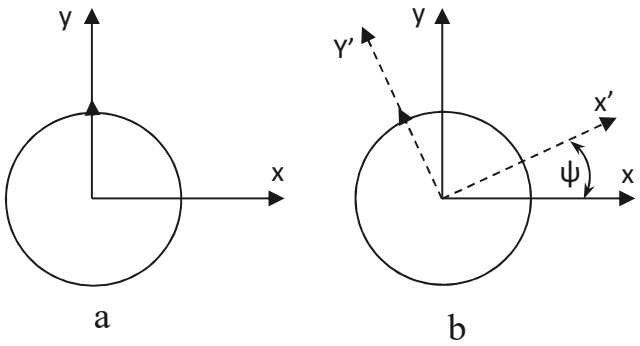

When the antenna is rotated by angle ψ, the orthogonal field components can be determined by projecting the rotated axes onto the parent coordinate system at z=0. The resulting field is

$$\boldsymbol{E}_{rot} = [\mathbf{x}\cos(\psi) - \mathbf{y}\sin(\psi) - j(\mathbf{x}\sin(\psi) + \mathbf{y}\cos(\psi))]\, e^{-j\beta z}\, e^{-j\omega t}$$

$$= (\mathbf{x}\, e^{-j\psi} - j\mathbf{y}\, e^{-j\psi})\, e^{-j\beta z}\, e^{-j\omega t}$$

$$= (\mathbf{x} - j\mathbf{y})\, e^{-j(\beta z+\psi)}\, e^{-j\omega t}$$

thereby preserving the RHCP wave and illustrating an additional phase (delay) of ψ radians.

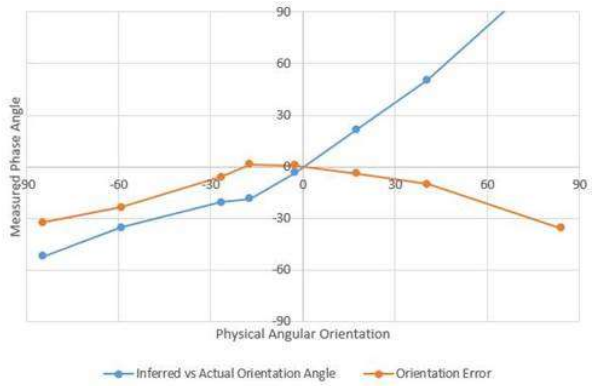

Long-Lived In-situ Solar System Explorer [6]

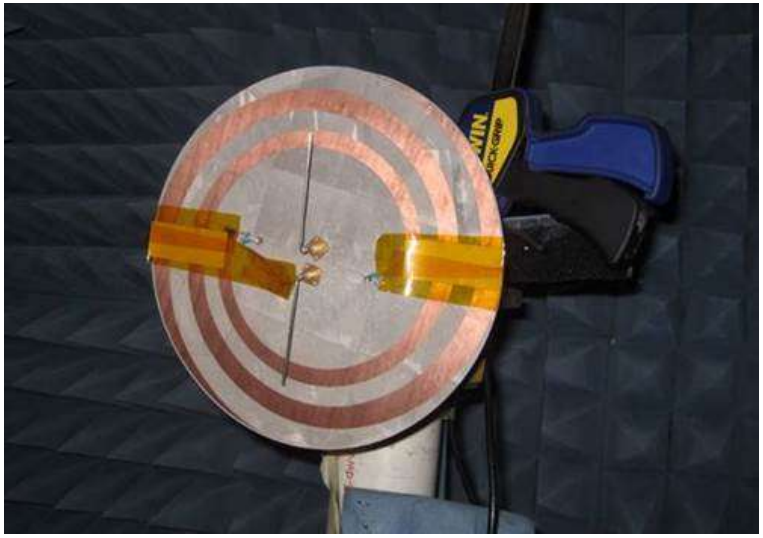

Logarithmic Spiral Low Axial Ratio Design. 24 cm spiral on high contrast substrate represents a factor of 11.4 reduction in physical size. The photograph shows the proof-of-concept integrated spiral and dipole (tuned to 640 MHz) at about a 90 degree rotation angle. Rotating the dipole causes essentially no phase shift variation. The standard deviation of the dipole phase shift as the dipole was rotated was only 0.9 degrees.

Inflatable Radome Antenna System [8]

The 2.5 m terrestrial radome antenna was manufactured by GATR (Huntsville, AL) and initially exhibited a 6 dB gain anomaly. GRC performed pattern measurements, surface scans using a laser radar system, and materials measurements and diagnosed several causes of the anomaly. Characterization was at Ku-band. Ultimately, measured directivity corresponded to 75 % of the theoretical gain from a perfect 2.5 meter aperture with uniform illumination.

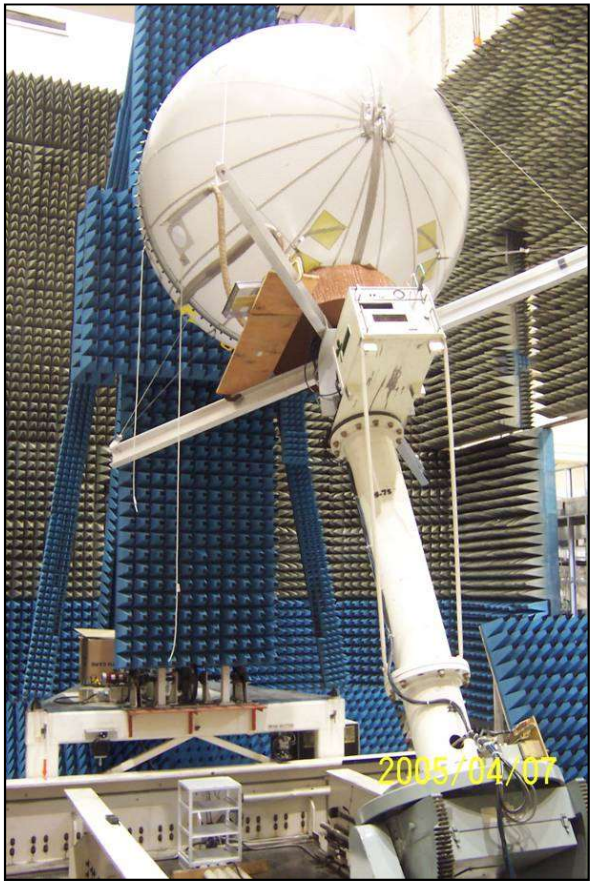

BB2.5 Radome Antenna on Pedestal Mount in the NASA GRC Near Field Range

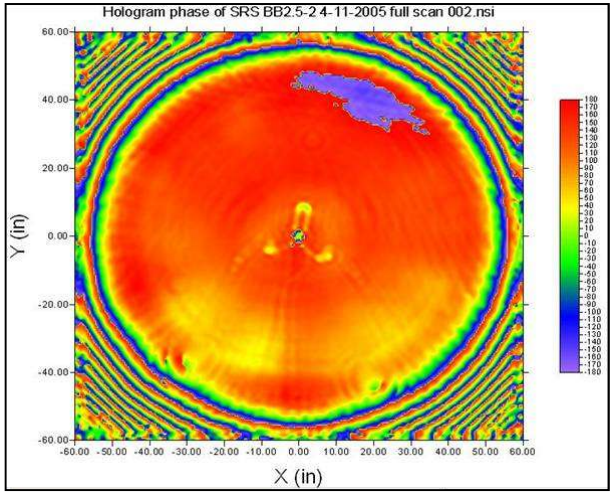

BB2.5 Radome Antenna Phase Hologram

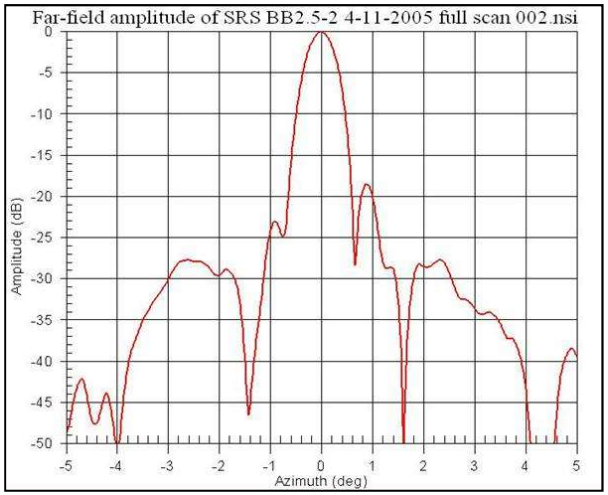

Measured far-field azimuth pattern

To date, GATR antennas have been deployed in six of the seven continents for humanitarian and disaster relief purposes. Here, The antenna provides communications in the search for a missing girl in San Diego, CA

Integrated Radio and Optical Communications "Teletenna [9]"

The goal of the iROC project is to integrate a 1550 nm optical terminal with a ≈3 m Ka-band antenna to form a resilient hybrid communications system for deep-space applications with the same mass as a conventional RF system.

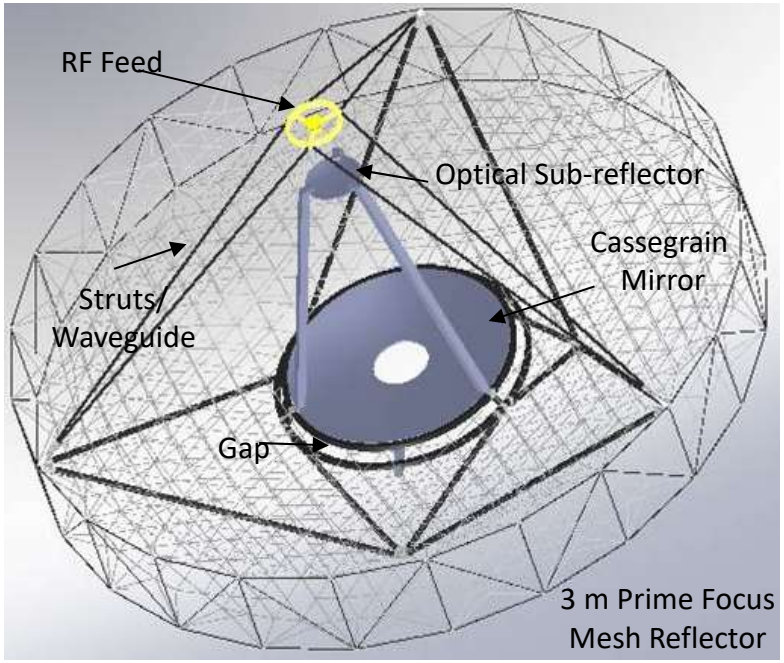

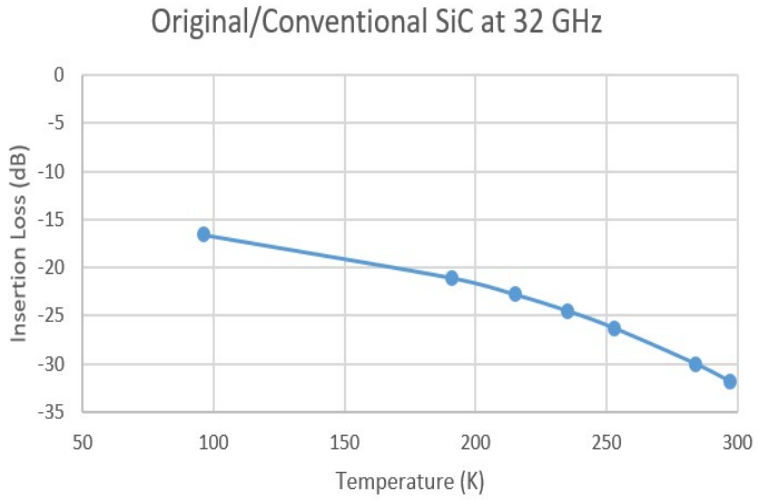

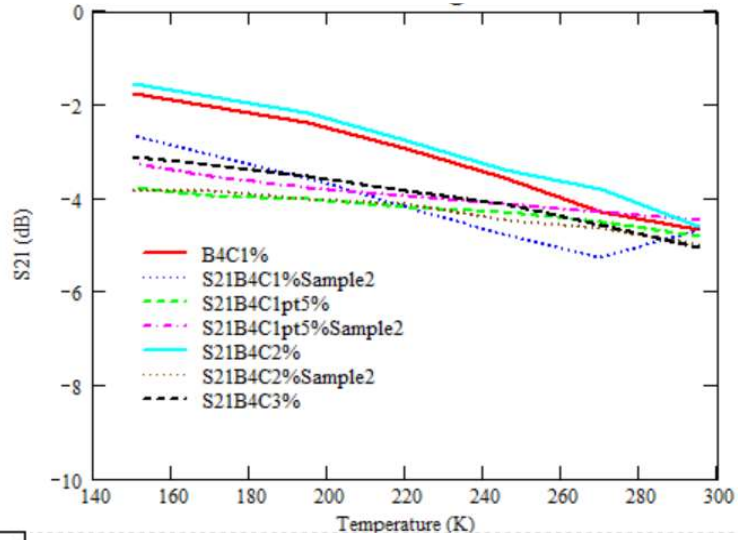

iROC Teletenna system:

- *3 m Ka-Band mesh reflector,*
- *A nominal 25 cm 1550nm optical aperture and associated vibration isolation platform.*
- *0.3 µradian star tracker accuracy (beacon-less pointing)*
- *4 µradian optical pointing requirement.*
- *Instantaneous data rates ≈350 MBPS from Mars perigee*

3 m Radio Antenna Material	25 cm Optical Mirror Material	Total Mass (kg)
Composite (16.7 kg)	Beryllium (0.8 kg)	17.5
Composite (16.7 kg)	Composite (0.2 kg)	16.9
Mesh (8.0 kg)	Composite (0.2 kg)	8.2

New type of SiC developed that retains all structural advantages but becomes translucent at Ka-band to enable novel hybrid teletenna systems, etc.

Cognitive Antennas

According to the FCC, a cognitive radio "can change its transmitter parameters based on interaction with the environment in which it operates." Hence we define a cognitive antenna as an environmentally perceptive antenna that can dynamically allocate bandwidth and/or adjust beam direction and directivity (beamwidth), EIRP, provide beam nulling, etc. to optimize spectral, spatial and temporal resources to complement cognitive radio technology. Intelligence is shared between the beam-forming controller and the radio cognitive engine.

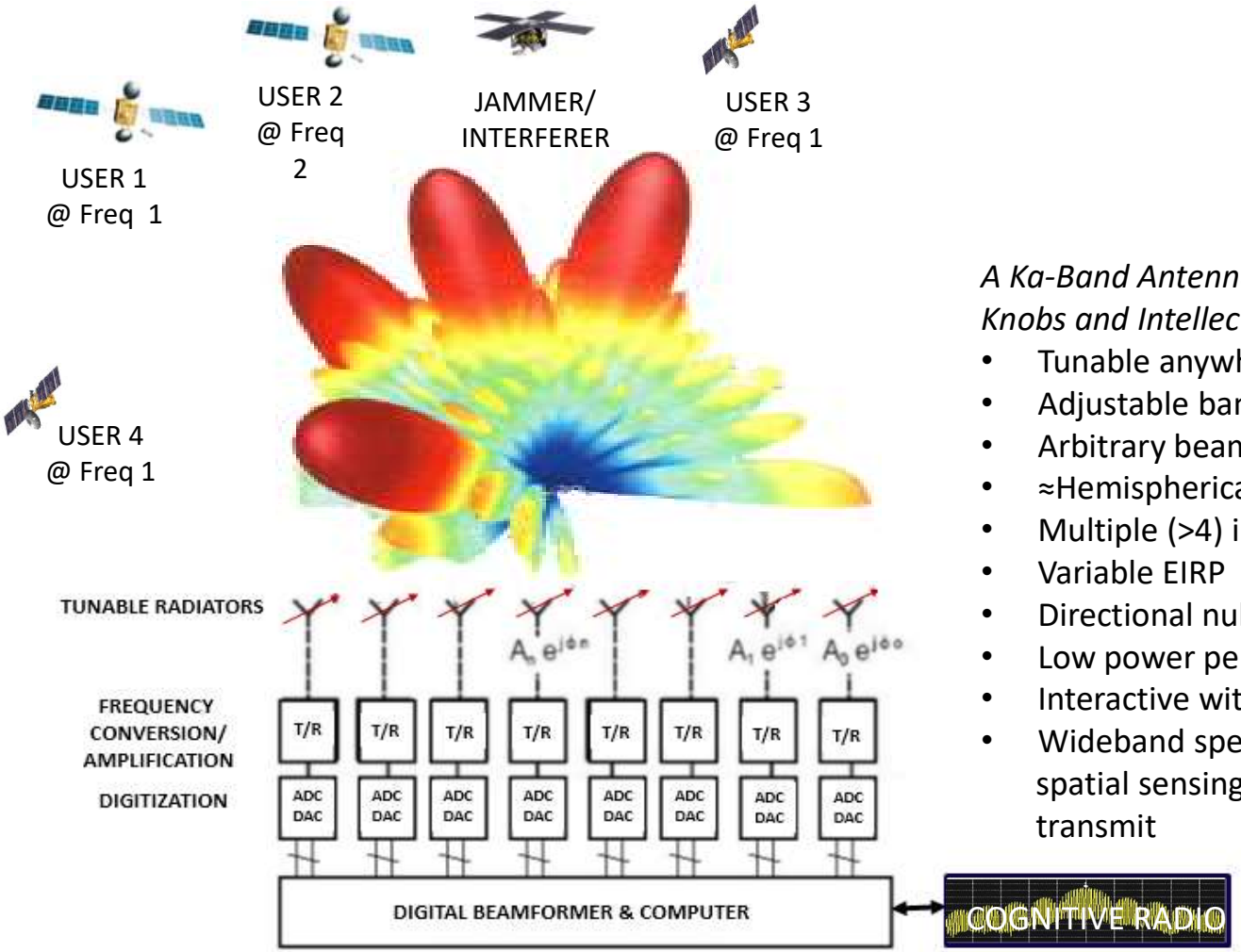

A Ka-Band Antenna with the Following Knobs and Intellect Does Not Exist:

- Tunable anywhere from ≈20 GHz to 33 GHz
- Adjustable bandwidth 10 MHz to 200 MHz
- Arbitrary beamwidth
- ≈Hemispherical coverage
- Multiple (>4) independent beams
- Variable EIRP
- Directional nulling
- Low power per channel (< 500 mW)
- Interactive with cognitive radio
- Wideband spectral and hemispherical spatial sensing and narrowband directional transmit

References

1. "Advances in Scanning Reflectarray Antennas Based on Thin Ferroelectric Film Phase Shifters," R. Romanofsky, Proc. IEEE, Special Issue on Technical Advances in Deep Space Communications and Tracking, Vol. 95, No. 10, Oct. 2007, pp. 1968-1975.

2. "How to Ensure Reliable Connectivity for Aerial Vehicles Over Cellular Networks", H.C. Nguyen, et al., IEEE Wireless Communications, Applications, Control and Modeling, Vol. 6, March, 2018, pp. 12304-12316.

3. "Broadband Directive Antenna for Cellular Control of Unmanned Aerial Vehicles", R. Romanofsky, To Be Published.

4. "Top-Hat Array for Zone Plate Antenna Feed," R. Romanofsky, Unpublished

5. "The Theoretical Precision with Which an Arbitrary Radiation Pattern may be Obtained from a Source of Finite Size," P. M. Woodward and J. D. Lawson, IEE-Part III: Radio and Communication Engineering, vol. 95, pp. 363–370, September 1948.

6. "Long-life In-situ Solar System Explorer (LLISSE) Probe Concept And Enabling High Temperature Electronics ," T. Kremic et al., Lunar and Planetary Science XLVIII, 2017, pp. 2986.

7. "Miniaturized Antenna System for Orientation Determination," R. Romanofsky, Subject of Invention Disclosure, NASA Glenn Research Center, 2019.

8. "Technology Benefiting Disaster Relief Has Roots in the SBIR Program and Technology Transfer Efforts," L. Stauber, Technology Transfer and Partnership Office, NASA's Glenn Research Center, 2014

9. "Near Earth and Deep Space Communications System," R. Romanofsky, Patent Pending, LEW 19485-1, 2017.